An introduction to hydrodynamic spin lattices

G. Pucci([1])([2])(*)

([1]) *Consiglio Nazionale delle Ricerche, Istituto di Nanotecnologia (CNR-Nanotec)*
    87036 Rende (CS), Italy
([2]) *Department of Mathematics, Massachusetts Institute of Technology - Cambridge, MA 02139,*
    USA

Summary. — This article is an introduction for non-specialist readers to hydrodynamic spin lattices, collections of macroscopic wave-propelled particles that exhibit symmetry-breaking phenomena. Hydrodynamic spin lattices have been introduced and thoroughly investigated with both experiments and theoretical models by Sáenz *et al.* (*Nature*, **596** (2021) 58). Here I summarize the main results obtained in experiments with one-dimensional lattices and describe the simplest theoretical model, *i.e.*, the generalized Kuramoto model, that captures the experimental data. The results presented here include transitions from antiferromagnetic to ferromagnetic order obtained by varying lattice geometry and system rotation, which is equivalent to applying a magnetic field. Finally, hydrodynamic spin lattices are briefly discussed in the context of active systems.

1. – Introduction

The coalescence of a liquid droplet with an underlying bath of the same liquid may be inhibited by forcing the bath to vibrate vertically [1]. The bath vibration sustains the drop to bounce on the bath's surface for a virtually infinite time with the intermediate of a thin air layer [2,3]. In some regimes, the drop moves horizontally across the surface by bouncing on the slope of the waves emitted by previous bounces [4-8] (fig. 1). The ensemble of drop and waves has been baptized a *walker*, which is a wave-particle association at the macroscopic scale [5]. Many configurations of the walker system have been explored to assess its potential and limitations as an analog of microscopic systems. These include interactions with slits [9-12], walls [13-16], cavities [17-20], bath bottom topography [13, 18, 21-23], and external forces [24-27]. Walkers exhibit several analogs with microscopic systems to various degrees of success [28], including quantization of

(*) E-mail: giuseppe.pucci@cnr.it
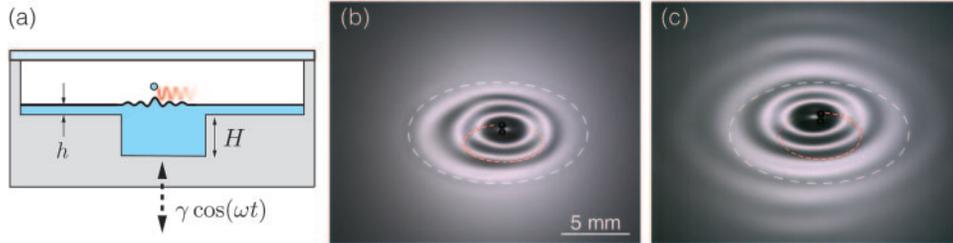
Fig. 1. – The behavior of a walking droplet confined by a submerged circular well. (a) Schematic cross section. (b) Snapshot with $h \ll 1\,\text{mm}$. (c) Snapshot with $h = 1\,\text{mm}$. Particle trajectories are indicated by red dashed lines and well boundaries in white. Figure from [21].

orbits [24,25,29] and angular momentum [26,30-32] in the presence of central forces, statistical switching between levels [25,27], level splitting [33], Hong-Ou-Mandel effect [34], spin states [35], wavelike particle statistics [17,36,37] and statistical projection effects [18] in corrals, and Friedel oscillations [22]. Collections of bouncing droplets exhibit features similar to crystal vibrations [38-41].

Collections of walkers are substantially more difficult to manipulate since walkers tend to coalesce with each other or with the bath or form bound states [42-48]. Until recently, the collective behavior of walkers (rather than bouncers) was investigated with limited configurations and particle numbers, specifically for exploring orbiting [4,43,46], promenading [45,47], ratcheting [42,49] and speed enhancement in walker strings [50]. The dynamics of walker pairs confined to a line has been shown to give rise to long-range correlations [51] and most recently to a hydrodynamic analog of superradiance [52]. Sáenz et al. [21,23] developed the first experimental design that enables the study of large collections of walkers coupled through the waves they emit, opening the door to the study of the collective motion of wave-driven particles.

2. – Experimental setup

Sáenz et al. tuned the bottom topography of the liquid bath to keep droplets separated whilst maintaining their wave-mediated interactions [20,21]. A submerged circular well may force a droplet to walk on a circular trajectory and thus 'spin' within the well (fig. 1). The extent of the walker wave field changes with the depth h of the liquid layer surrounding the well: small depth ($h \ll 1\,\text{mm}$) results in strongly confined waves (fig. 1(b)) while a larger depth ($h \approx 1\,\text{mm}$) allows the waves to escape the well over a few wavelengths (fig. 1(c)).

Hydrodynamic spin lattices are made of multiple walking droplets, each confined by a submerged circular well to 'spin' on the bath surface and interacting with the neighbors via the waves it emits (fig. 2(a), (b)). The liquid used was silicone oil with density $\rho = 950\,\text{kg m}^{-3}$, viscosity $\nu = 20.9\,\text{cSt}$, and surface tension $\sigma = 20.6\,\text{mN m}^{-1}$. The well depth was $H = 6.2\,\text{mm}$, which corresponds to "infinite" depth with respect to the characteristic wavelength of the system. The bath was forced by an electromagnetic shaker to oscillate vertically with acceleration $\Gamma(t) = \gamma \cos 2\pi f t$, where $\gamma < \gamma_F$ is the acceleration amplitude, with γ_F the Faraday instability threshold [53,54], f is the frequency, and t is time. Drops had a diameter $D_d = 0.75 \pm 0.01\,\text{mm}$ and bounced in phase at half the forcing frequency. Therefore, they were local triggers of the Faraday instability and excited approximately
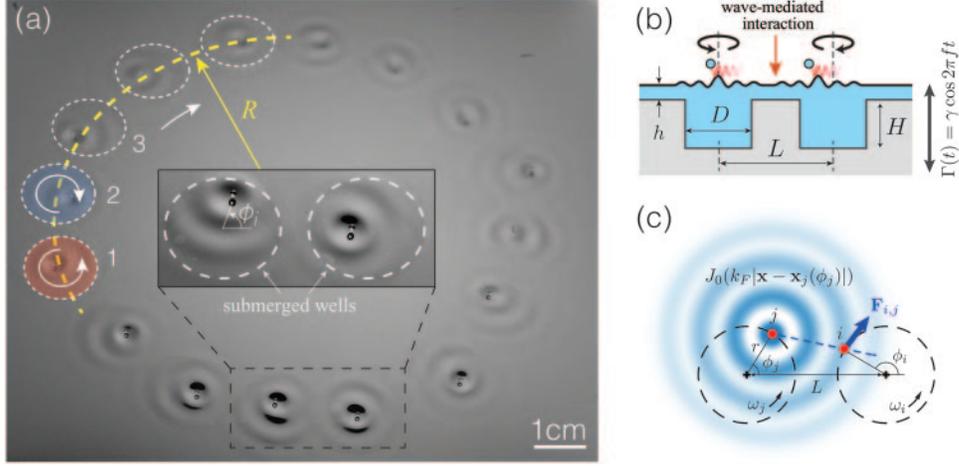
Fig. 2. – 1D lattice and wave-mediated interactions. (a) Oblique view of a ring of submerged circular wells with walking droplets. The fluid layer between wells allows for wave-mediated interaction between neighboring drops. (b) Schematic cross section of two interacting drops. (c) Schematic representation of the model of two interacting drops. Material from [23].

standing circular waves with wavelength λ_F. Droplets were tracked with an in-house algorithm that served to measure the spin $S(t) = L_z(t)/m$ of each droplet, where m is the droplet's mass, and L_z is the angular momentum with respect to the well center. Experiments were started with random initial spin configurations and run for several hours to achieve statistical significance. The bath was enclosed inside a transparent chamber to ensure isolation from ambient air currents.

3. – Generalized Kuramoto model

Starting from first principles, Sáenz *et al.* demonstrated that the simplest model capable of describing the collective behavior in hydrodynamic spin lattices is a phase oscillator model [23] (fig. 2(c)). Walker trajectories are assumed to be circular $\mathbf{x}_i(t) = r_0(\cos\phi_i(t), \sin\phi_i(t))$, where (r_0, ϕ_i) are the cylindrical coordinates describing the position of droplet i with respect to the center of the well in which it walks, and $\omega_i = \dot{\phi}_i$ is the angular frequency of rotation of the droplet. Since walking droplets have a preferred walking speed [5,7], which we denote with v_0, preferred orbital frequencies are defined as $\pm\omega_0 = \pm v_0/r_0$. The presence of a preferred orbital frequency is modeled by a non-linear Rayleigh-type friction, leading to the following equation:

$$(1) \qquad \dot{\omega}_i = \frac{1}{\tau}\left(1 - \frac{\omega_i^2}{\omega_0^2}\right)\omega_i + \sum_j F_{ij}(\phi_i, \phi_j),$$

where F_{ij} is the wave-mediated force exerted on drop i by its nearest neighbor j, and τ is the timescale over which perturbations to ω_0 decay. Assuming weak accelerations and small orbital radii $r_0 \ll L$ in the droplet motion, the interaction force can be derived

from a coupling potential

$$(2a) \qquad F_{ij}(\phi_i, \phi_j) = -\frac{\partial U}{\partial \phi_i},$$

$$(2b) \qquad U(\phi_i, \phi_j) = \frac{1}{2}\alpha(\cos\phi_i - \cos\phi_j)^2 + \frac{1}{2}\beta(\sin\phi_i - \sin\phi_j)^2.$$

Here $\alpha \propto J_0''(k_F L)$ and $\beta \propto J_0'(k_F L)$, where $J_0(k_F(|\mathbf{x} - \mathbf{x}_j|))$ is a Bessel function of the first kind centered at the position of the neighboring drop that approximates the coupling wave field, and $k_F = 2\pi/\lambda_F$.

4. – Order parameters

Collective order was characterized by measuring three parameters. The normalized "magnetization"

$$(3) \qquad M(t) = \frac{\sum_i S_i(t)}{\sum_i |S_i(t)|}$$

quantifies the global symmetry breaking, with $\sum_i$ indicating a sum over all N spins and $S_i(t)$ the spin of droplet i. The normalized spin-spin correlation

$$(4) \qquad \chi(t) = \frac{\sum_{i \sim j} S_i(t)S_j(t)}{\sum_{i \sim j} |S_i(t)S_j(t)|}$$

quantifies pairwise symmetry breaking, with $i \sim j$ indicating that the sum is done over adjacent pairs. Negative χ corresponds to average counter-rotation of adjacent walkers (antiferromagnetic behavior), while positive χ corresponds to average co-rotation of adjacent walkers (ferromagnetic behavior). The third order parameter characterized by Sáenz et al. [23] is the average phase difference of rotation of adjacent walkers, which will not be discussed here.

5. – Collective behavior as a function of forcing

In the first series of experiments, the lattice spacing L was fixed and the dependence of the collective behavior on the forcing acceleration γ/γ_F was explored (fig. 3). γ/γ_F is somewhat a tuning parameter for the extension of the walker wave field since higher forcing results in waves lasting for a longer time on the bath's surface [6]. In our experiments, the average magnetization was observed to vanish, $\langle M \rangle \approx 0$, while the average spin-spin correlation $\langle \chi \rangle$ exhibited a monotonic dependence on the forcing acceleration. Specifically, $\langle \chi \rangle \approx 0$ at low γ/γ_F due to limited extensions of the wave field and thus the lack of wave-mediated interactions. The spin-spin correlation decreased with the forcing, as a result of increasing wave-mediated interactions, and reached a minimum value roughly corresponding to the maximum amplitude at which an isolated spinning drop would have a stable circular trajectory. Further increasing of γ/γ_F corresponds to increasing $\langle \chi \rangle$ back to zero, presumably because the strong wave-mediated interactions 'randomize' the collective behavior. The generalized Kuramoto model captures the observed behavior well despite the significant approximations (fig. 3).
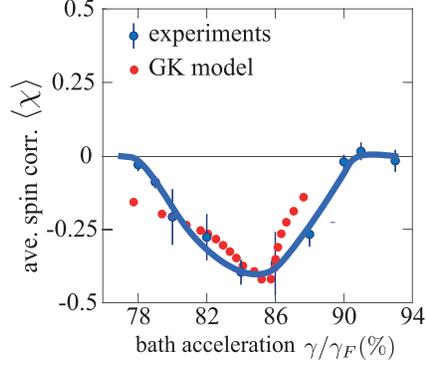
Fig. 3. – Dependence of the average spin-spin correlation $\langle \chi \rangle$ on the forcing acceleration amplitude γ/γ_F in experiments and as predicted by the Generalized Kuramoto model for a 1D lattice. Experimental parameters: $N = 20$ wells, $L = 17.7\,\text{mm}$, $D = 14\,\text{mm}$, $h = 1\,\text{mm}$, $f = 80\,\text{Hz}$, $\lambda_F = 4.75\,\text{mm}$ and $\gamma_F = 4.780\,\text{g}$. Material from [23].

6. – Collective behavior as a function of spacing

Sáenz *et al.* [23] then proceeded to explore the dependence of the spin-spin correlation on the lattice spacing L. Experimentally, two lattice spacings were explored, leading to
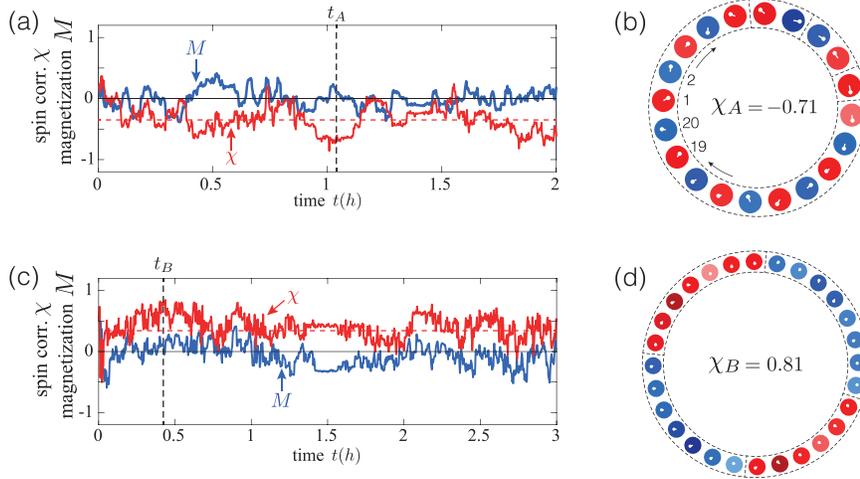
Fig. 4. – Antiferromagnetic and ferromagnetic order of 1D lattices. (a) Time evolution of spin-spin correlation χ and magnetization M of a 1D spin lattice with $N = 20$ wells, $L = 17.7\,\text{mm}$, $D = 14\,\text{mm}$, $H = 1\,\text{mm}$, $f = 80\,\text{Hz}$, $\lambda_F = 4.75\,\text{mm}$ and $\gamma/\gamma_F = 82\%$ with $\gamma_F = 4.780\,\text{g}$. (b) Snapshot of the collective *antiferromagnetic* order as it appeared at instant t_A in (a), where χ_A is the corresponding spin-spin correlation. (c) Time evolution of spin-spin correlation χ and magnetization M of a 1D spin lattice with $N = 28$ wells, $L = 13.2\,\text{mm}$, $D = 10\,\text{mm}$, $H = 0.8\,\text{mm}$, $f = 78\,\text{Hz}$, $\lambda_F = 4.84\,\text{mm}$ and $\gamma/\gamma_F = 86\%$ with $\gamma_F = 5.280\,\text{g}$. (d) Snapshot of the collective *ferromagnetic* order as it appeared at instant t_B in (c), where χ_B is the corresponding spin-spin correlation. Material from [23].

either antiferromagnetic (fig. 4(a),(b)) or ferromagnetic (fig. 4(c),(d)) order. This behavior is captured by the generalized Kuramoto model, which also shows that continuous transitions from antiferromagnetic to ferromagnetic order and vice versa can be obtained by varying L. The model also provides a simple theoretical framework: antiferromagnetic or ferromagnetic pairwise modes are selected by minimizing the potential U in eq. (2) (see *Methods* in Sáenz *et al.* [23] for the underlying mechanism).

7. – Applying the equivalent of a magnetic field

Finally, Sáenz *et al.* proceeded to apply the equivalent of a magnetic field [23]. It is known that an antiferromagnetic material can become ferromagnetic if a constant magnetic field is applied. To apply an equivalent of the magnetic field they used the analogy between the Lorentz force $\mathbf{F}_B = q(\mathbf{v} \times \mathbf{B})$ acting on a charge q that moves with velocity $\mathbf{v}$ and the Coriolis force $\mathbf{F}_\Omega = m(\mathbf{v} \times 2\mathbf{\Omega})$ acting on a mass m that moves with velocity $\mathbf{v}$ in a frame that rotates with constant angular velocity $\mathbf{\Omega}$ [24]. A lattice with initial antiferromagnetic order was rotated anticlockwise, and a polarization to ferromagnetic order was observed (fig. 5(a)). Correspondingly, the magnetization moved from zero to a positive value. When the direction of rotation was inverted, the lattice remained ferromagnetic, but the magnetization changed to negative (fig. 5(a), (b)). Spins generally aligned with the "magnetic" field, that is, the bath angular velocity vector. The mechanism underlying this "magnetization" lies in the capacity of the Coriolis force to destabilize circular trajectories. A bath co-rotating with a drop gave rise to a Coriolis force that opposed the confining force of the well, thus preserving the circular trajectory and increasing its radius. A bath counter-rotating with a drop gave rise to a Coriolis force that pointed inwards and destabilized circular orbits into trefoil-like trajectories, through which the direction of rotation of the drop could be easily reversed by the perturbations from neighboring drops. The experimental results are captured by the
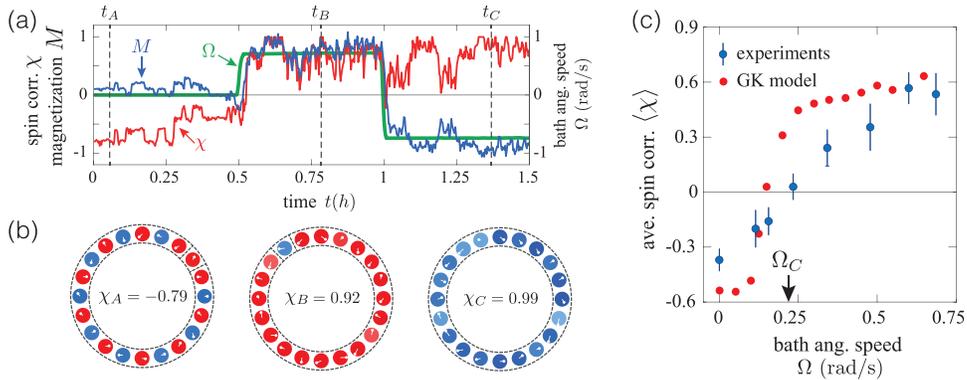
Fig. 5. – Effect of applying an equivalent magnetic field via system rotation. (a) Time evolution of spin-spin correlation χ and magnetization M initially without rotation, ($\Omega = 0$) and then with anticlockwise ($\Omega = 0.7$ rad s^{-1}) and clockwise ($\Omega = -0.7$ rad s^{-1}) rotation. (b) Configurations at instants t_A, t_B and t_C in (a). (c) Average spin-spin correlation as a function of the system angular speed in experiments and as it results from the Generalized Kuramoto model with rotation. Experimental parameters are the same as in fig. 3 with $\gamma/\gamma_F \approx 85\%$. Material from [23].

generalized Kuramoto model in eq. (1) by adding the Coriolis force (fig. 5(c)). The polarization to ferromagnetic order occurred at a supercritical rotation rate Ω_C in both experiments and theoretical modeling.

8. – Conclusion and perspective work

In this communication, I have summarized the results obtained by Sáenz *et al.* on 1D hydrodynamic spin lattices, which are lattices of drops propelled by waves on the surface of a liquid [23]. Sáenz *et al.* also explored the behavior of 2D square and triangular lattices. Specifically, they observed a transition from antiferromagnetic to ferromagnetic order and global magnetization with bath rotation in square lattices. They also found ferromagnetic domains in 2D square lattices by varying the lattice spacing in simulations. The effect of the bouncing phase of the drops was investigated, and it was found that lattices with all drops bouncing in phase maximize $|\langle\chi\rangle|$. Details of spin flips were also reported. All these results demonstrate the plethora of configurations that can be designed and explored with spin lattices of walking drops, which may lead, for instance, to the hydrodynamic analog of spin-wave dynamics [55] and Anderson localization [56].

It is worth mentioning the potential impact of hydrodynamic spin lattices on the statistical physics of active systems. Active systems are composed of self-driven units capable of consuming energy to move or exert forces on each other [57, 58]. These systems have recently attracted the attention of physicists for the possibility of extending the framework of statistical physics to incorporate non-equilibrium phenomena. Extensive studies have been devoted to overdamped active systems (see for instance [58]) in which interactions are mediated by viscous hydrodynamic forces that decay monotonically with distance, and inertial active systems (see for example [59]), which exhibit spatiotemporally complex interactions and are relatively less understood. Hydrodynamic spin lattices are a rare example of an active system in which both dissipation and inertia are at play and thus promise a number of novel collective behaviors, some of which have been anticipated in recent reviews [60, 61]. Furthermore, and maybe more interestingly, hydrodynamic spin lattices are the first example of an active system with wave-mediated interactions, in which interaction forces are long-range and spatially-oscillatory, *i.e.*, defined by alternating regions of attraction and repulsion. Recent experiments on wave-propelled solid particles on a fluid interface show that wave-mediated interactions lead to the multistability of a discrete set of interactions states [62], which contribute to increasing the number of collective behaviors that can be studied in these systems.

<p align="center">* * *</p>

are coming in the future since this system continues to show its potential and unveil mysteries.

REFERENCES

[1] WALKER J., *Sci. Am.*, **238** (1978) 151.
[2] COUDER Y., FORT E., GAUTIER C. H. and BOUDAOUD A., *Phys. Rev. Lett.*, **94** (2005) 1.
[3] MOLÁČEK J. and BUSH J. W. M., *J. Fluid Mech.*, **727** (2013) 612.
[4] COUDER Y., PROTIÈRE S., FORT E. and BOUDAOUD A., *Nature*, **437** (2005) 208.
[5] PROTIÈRE S., BOUDAOUD A. and COUDER Y., *J. Fluid Mech.*, **554** (2006) 85.
[6] EDDI A., SULTAN E., MOUKHTAR J., FORT E., ROSSI M. and COUDER Y., *J. Fluid Mech.*, **674** (2011) 433.
[7] MOLÁČEK J. and BUSH J. W. M., *J. Fluid Mech.*, **727** (2013) 612.
[8] BUSH J. W., *Annu. Rev. Fluid Mech.*, **47** (2015) 269.
[9] COUDER Y. and FORT E., *Phys. Rev. Lett.*, **97** (2006) 1.
[10] ANDERSEN A., MADSEN J., REICHELT C., ROSENLUND AHL S., LAUTRUP B., ELLEGAARD C., LEVINSEN M. T. and BOHR T., *Phys. Rev. E*, **92** (2015) 1.
[11] PUCCI G., HARRIS D. M., FARIA L. M. and BUSH J. W. M., *J. Fluid Mech.*, **835** (2018) 1136.
[12] ELLEGAARD C. and LEVINSEN M. T., *Phys. Rev. E*, **102** (2020) 023115.
[13] EDDI A., FORT E., MOISY F. and COUDER Y., *Phys. Rev. Lett.*, **102** (2009) 3.
[14] PUCCI G., SÁENZ P. J., FARIA L. M. and BUSH J. W. M., *J. Fluid Mech.*, **804** (2016) R3.
[15] HARRIS D. M., BRUN P.-T., DAMIANO A., FARIA L. M. and BUSH J. W. M., *Chaos*, **28** (2018) 096105.
[16] TADRIST L., GILET T., SCHLAGHECK P. and BUSH J. W. M., *Phys. Rev. E*, **102** (2020) 013104.
[17] HARRIS D. M., MOUKHTAR J., FORT E., COUDER Y. and BUSH J. W. M., *Phys. Rev. E*, **88** (2013) 1.
[18] SÁENZ P. J., CRISTEA-PLATON T. and BUSH J. W. M., *Nat. Phys.*, **14** (2018) 315.
[19] FILOUX B., HUBERT M., SCHLAGHECK P. and VANDEWALLE N., *Phys. Rev. Fluids*, **2** (2017) 013601.
[20] CRISTEA-PLATON T., SÁENZ P. J. and BUSH J. W., *Chaos*, **28** (2018) 096116.
[21] SÁENZ P. J., PUCCI G., GOUJON A., CRISTEA-PLATON T., DUNKEL J. and BUSH J. W. M., *Phys. Rev. Fluids*, **3** (2018) 100508.
[22] SÁENZ P. J., CRISTEA-PLATON T. and BUSH J. W. M., *Sci. Adv.*, **6** (2020) eaay9234.
[23] SÁENZ P. J., PUCCI G., TURTON S. E., GOUJON A., ROSALES R. R., DUNKEL J. and BUSH J. W. M., *Nature*, **596** (2021) 58.
[24] FORT E., EDDI A., BOUDAOUD A., MOUKHTAR J. and COUDER Y., *Proc. Natl. Acad. Sci. U.S.A.*, **107** (2010) 17515.
[25] HARRIS D. M. and BUSH J. W. M., *J. Fluid Mech.*, **739** (2013) 444.
[26] PERRARD S., LABOUSSE M., MISKIN M., FORT E. and COUDER Y., *Nat. Commun.*, **5** (2014) 3219.
[27] PERRARD S., LABOUSSE M., FORT E. and COUDER Y., *Phys. Rev. Lett.*, **113** (2014) 104101.
[28] BUSH J. W. M. and OZA A. U., *Rep. Prog. Phys.*, **84** (2021) 017001.
[29] OZA A. U., HARRIS D. M., ROSALES R. R. and BUSH J. W. M., *J. Fluid Mech.*, **744** (2014) 404.
[30] LABOUSSE M., PERRARD S., COUDER Y. and FORT E., *New J. Phys.*, **16** (2014) 113027.
[31] KURIANSKI K. M., OZA A. U. and BUSH J. W. M., *Phys. Rev. Fluids*, **2** (2017) 113602.
[32] DUREY M. and MILEWSKI P. A., *J. Fluid Mech.*, **821** (2017) 296.
[33] EDDI A., MOUKHTAR J., PERRARD S., FORT E. and COUDER Y., *Phys. Rev. Lett.*, **108** (2012) 1.

[34] VALANI R. N., SLIM A. C. and SIMULA T., *Chaos*, **28** (2018) 096104.
[35] OZA A. U., ROSALES R. R. and BUSH J. W. M., *Chaos*, **28** (2018) 096106.
[36] GILET T., *Phys. Rev. E*, **93** (2016) 042202.
[37] DUREY M., MILEWSKI P. A. and BUSH J. W. M., *Chaos*, **28** (2018) 096108.
[38] EDDI A., BOUDAOUD A. and COUDER Y., *EPL*, **94** (2011) 20004.
[39] THOMSON S. J., COUCHMAN M. M. P. and BUSH J. W. M., *Phys. Rev. Fluids*, **5** (2020) 083601.
[40] BARNES L., PUCCI G. and OZA A. U., *C. R-Méc.*, **348** (2020) 573.
[41] COUCHMAN M. M. P. and BUSH J. W. M., *J. Fluid Mech.*, **903** (2020) A49.
[42] EDDI A., TERWAGNE D., FORT E. and COUDER Y., *EPL*, **82** (2008) 44001.
[43] PROTIÈRE S., BOHN S. and COUDER Y., *Phys. Rev. E*, **78** (2008) 1.
[44] WIND-WILLASSEN Ø., MOLÁČEK J., HARRIS D. M. and BUSH J. W. M., *Phys. Fluids*, **25** (2013) 082002.
[45] BORGHESI C., MOUKHTAR J., LABOUSSE M., EDDI A., FORT E. and COUDER Y., *Phys. Rev. E*, **90** (2014) 1.
[46] OZA A. U., SIÉFERT E., HARRIS D. M., MOLÁČEK J. and BUSH J. W. M., *Phys. Rev. Fluids*, **2** (2017) 053601.
[47] ARBELAIZ J., OZA A. U. and BUSH J. W. M., *Phys. Rev. Fluids*, **3** (2018) 013604.
[48] COUCHMAN M. M. P., TURTON S. E. and BUSH J. W. M., *J. Fluid Mech.*, **871** (2019) 212.
[49] COUCHMAN M. M. P., CALDAIROU P. and BUSH J. W. M., *Chaos*, **28** (2018) 096112.
[50] FILOUX B., HUBERT M. and VANDEWALLE N., *Phys. Rev. E*, **92** (2015) 041004.
[51] NACHBIN A., *Chaos*, **28** (2018) 096110.
[52] PAPATRYFONOS K., RUELLE M., BOURDIOL C., NACHBIN A., BUSH J. W. M. and LABOUSSE M., *Hydrodynamic superradiance in wave-mediated cooperative tunneling*, to be published in *Commun. Phys.* (2022).
[53] FARADAY M., *Philos. Trans. R. Soc. London*, **121** (1831) 299.
[54] DOUADY S., *J. Fluid Mech.*, **221** (1990) 383.
[55] CHUMAK A. V., VASYUCHKA V., SERGA A. and HILLEBRANDS B., *Nat. Phys.*, **11** (2015) 453.
[56] LAGENDIJK A., TIGGELEN B. V. and WIERSMA D. S., *Phys. Today*, **62** (2009) 24.
[57] RAMASWAMY S., *Annu. Rev. Condens. Matter Phys.*, **1** (2010) 323.
[58] MARCHETTI M. C., JOANNY J. F., RAMASWAMY S., LIVERPOOL T. B., PROST J., RAO M. and SIMHA R. A., *Rev. Mod. Phys.*, **85** (2013) 1143.
[59] CAVAGNA A., GIARDINA I. and GRIGERA T. S., *Phys. Rep.*, **728** (2018) 1.
[60] BECHINGER C., DI LEONARDO R., LÖWEN H., REICHHARDT C., VOLPE G. and VOLPE G., *Rev. Mod. Phys.*, **88** (2016) 045006.
[61] KLOTSA D., *Soft Matter*, **15** (2019) 8946.
[62] HO I., PUCCI G., OZA A. U. and HARRIS D. M., *Capillary surfers: wave-driven particles at a fluid interface*, arXiv:2102.11694v2 (2021).